Investigations of Double Proton Transfer Behavior between Glycinamide and Formamide Using Density Functional Theory

Ping Li[†,‡] and Yuxiang Bu*[,†,‡]

Institute of Theoretical Chemistry, Shandong University, Jinan 250100, P. R. China, and Department of Chemistry, Qufu Normal University, Qufu 273165, P. R. China

Received: April 4, 2004; In Final Form: June 28, 2004

The behaviors of double proton transfer (DPT) between two model peptide compounds, that is, glycinamide and formamide, have been investigated employing the B3LYP/6-311++G** level of theory. Thermodynamic and especially kinetic parameters, such as tautomeric energy, equilibrium constant, and barrier heights, have been discussed. The relevant quantities involved in the DPT process, such as geometrical changes, interaction energies, and the intrinsic reaction coordinate (IRC) calculations, have also been studied. Contrary to those tautomeric processes directly assisted with one, two, and three water molecules, the participation of a formamide molecule disfavors the tautomeric process for both glycinamide and formamide thermodynamically compared with their direct tautomeric cases. The DPT process proceeds with a concerted mechanism rather than a stepwise one since no ion-pair complexes have been located during the PT process. The barrier heights are 20.45 and 0.70 kcal/mol for the forward and reverse directions, respectively. However, both of them have been reduced by 3.47 and 3.07 kcal/mol to 16.98 and −2.37 kcal/mol with further inclusion of zero-point vibrational energy (ZPVE) corrections, which has been further reproduced by the full optimizations at the MP2(FULL)/6-311++G** level of theory. Additionally, the solvent effects on the thermodynamic and kinetic processes have been predicted qualitatively employing the IPCM model within the framework of the self-consistent reaction field (SCRF) theory. More importantly, the reliability of the B3LYP/6-311++G** level of theory in exploring the DPT phenomena in the glycinamide complexes has been confirmed for future study.

1. Introduction

As one of the simplest and the most fundamental phenomena in the tautomeric equilibrium and oxidation−reduction reactions, intra- or intermolecular proton transfers (PTs) play an important role in many chemical and biochemical processes.[1−3] A large number of theoretical and experimental studies have been carried out to enrich the information regarding the possible mechanisms of PTs, tautomeric equilibria, and relevant properties associated with PT processes.[1−47] Relatively, multiproton transfer phenomena, in which more than one proton is transferred with a concerted or stepwise mechanism, have not been studied as extensively as the reactions of single proton transfer though they play an important role in the proton relay occurring in enzymatic reactions, transport phenomena in biological membrane, and DNA mutations besides the fact that they are also implicated in the charge-relay mechanism of hydrolyses catalyzed by enzymes and other enzyme- and water-catalyzed tautomeric processes.[3] In the present study, a prototype of double proton transfer (DPT) occurring between two model peptide compounds, glycinamide and formamide, has been investigated at the B3LYP/6-311++G** level of theory to get some useful information about the nature of the mechanism in multiproton transfer processes. In addition to the interaction energies and geometrical changes upon complexation, discussions will focus mainly on the thermodynamic and kinetic features, including tautomeric energy, barrier heights, and the mechanism of DPT. Additionally, MP2(FULL)/6-311++G** level of theory has been employed to further rationalize the magnitude of the barrier height for the reverse reaction.

As one of the important components in glycinamide ribonucleotide synthetase, the relevant investigations of glycinamide have been reported previously theoretically and experimentally.[48−56] For example, the formations of the peptide bond in glycinamide uncatalyzed or catalyzed by the metal cations or ammonia have been extensively studied.[48−50] Klassen et al. reported the collision-induced dissociation threshold energies of protonated glycinamide determined with a modified triple quadrupole mass spectrometer.[51] The unimolecular chemistry of protonated glycinamide and its proton affinity determined by mass spectrometric experiments and theoretical model were reported by Kinser et al.[52] The interrelationship between conformations and theoretical chemical shift was investigated by Sulzbach et al.,[53] in which some useful conformational information was mentioned using the restricted Hartree−Fock (RHF) theory and 6-31G* basis set. Ramek et al. discussed the basis-set influence on the nature of the conformations of glycinamide (minimum or saddle point) in ab initio self-consistent field (SCF) calculations.[54] Recently, multiply sodiated ions were observed by electron-spraying glycinamide and their N-acetylated and O-amidated derivatives in the presence of sodium hydroxide, in which some sodiated glycinamide conformers were obtained at the B3LYP/6-311++G** level of theory.[55] The possible conformers of glycinamide in the gas phase and in solution had been systematically explored by us, where three pairs of mirror-image conformers and one *Cs*

* Corresponding author. E-mail: byx@sdu.edu.cn.
† Shandong University.
‡ Qufu Normal University.

10.1021/jp048527b CCC: $27.50 © 2004 American Chemical Society
Published on Web 10/20/2004

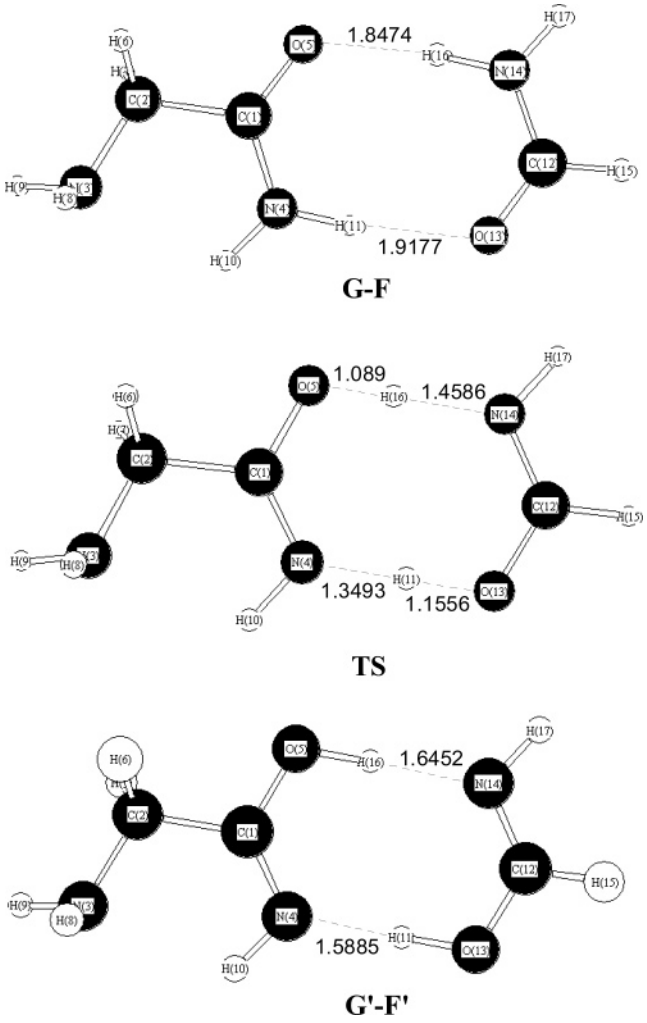

Figure 1. Optimized complex of glycinamide with formamide and its tautomeric product together with the transition state connecting them.

conformer had been located on the global potential energy surface (PES) of glycinamide at the B3LYP/6-311++G** level of theory.[56a,56b] Its acid−base behaviors, ionization potentials, and electron affinities in the gas phase and in solution had also been predicted,[56c,56d] where the calculated proton affinity for the global minimum, 216.81 kcal/mol, is well consistent with the experimental value 217.23 kcal/mol.[52] Additionally, the PT from the amide N to carbonyl O atom with and without water-assisted cases have also been investigated recently.[56e] In those studies,[56] the reliability of the B3LYP/6-311++G** level of theory has been verified through comparisons with the experimental data available and the higher-level calculations including MP2, MP3, MP4(SDQ), and CCSD(T) levels.

2. Computational Details

Using the global minimum of glycinamide as a starting point,[56a] the selected geometries have been fully optimized without any symmetry constraints, where glycinamide and formamide interact with each other by means of a pair of two parallel intermolecular H-bonds as displayed in Figure 1 since what we are most concerned with is the DPT occurring between them. At the same time, this interaction mode may be the most favorable one among the possible modes and is representative in mostly biological systems, such as the interactions between base pairs and other model systems studied previously.[5h,10a,17e,18a,18b] Of course, many complexes between glycinamide and formamide can be formed through the other H-bond interactions. Here, the three geometries associated with the DPT are denoted as **G**−**F**, **TS**, and **G′-F′** for the sake of simplicity. Normal-mode analyses have been performed to verify that the stable complexes have all positive frequencies and the transition state has only one imaginary frequency with the corresponding eigenvector pointing toward the reactants and products, where none of these frequencies have been scaled because of the ability of DFT calculations to predict them accurately as proposed by Johnson et al.[57] To estimate the effect of ZPVE corrections on the calculated potential energy curve along the reaction coordinates, the frequencies of the non-stationary points during the intrinsic reaction coordinate (IRC)[58] have been projected out and all other modes are constrained to be orthogonal to the gradient vector. Furthermore, the IRC calculations in the mass-weighted internal coordinates with a stepsize of 0.1 amu$^{1/2}$ bohr have also been performed to further confirm the validity of the transition states (TSs) connecting the reactants and products. Here, the direction of the DPT from **G**−**F** to **G′**−**F′** is defined as the forward reaction and the reverse one is the reaction in the opposite direction.

As mentioned above, the density functional method adopted here is B3LYP,[59,60] that is, Becke's three-parameter hybrid functional using the Lee−Yang−Parr correlation function. The 6-311++G**, which is a triple-ζ basis set including diffuse and polarization functions on both heavy and hydrogen atoms, is used throughout the calculations since its reliability has been verified as mentioned above. To further rationalize the magnitude of the barrier height for the reverse reaction, we have also reoptimized the whole stationary points employing the MP2-(FULL)/6-311++G** level of theory. On the basis of the B3LYP-optimized geometries, single-point energy calculations have also been performed to improve the energetic quantities at the higher-level calculations including second-, third-, and fourth-order Møller−Plesset theory (abbreviated as MP2, MP3, and MP4SDQ), and coupled cluster method (CCSD(T)) including the single, double, and perturbative triple excitation including all the electron correlations.

To investigate how the presence of solvent molecules affects the relevant quantities associated with the PT processes qualitatively, the isodensity surface polarized continuum model (IPCM),[61,62] which has been successful in the descriptions of many chemical systems in solution,[63−65] has been employed. These calculations are performed at the B3LYP/6-311++G** level of theory on the basis of the optimized gas-phase structures in a series of solutions, such as chloroform, dichloroethane, and water (the dielectric constants ϵ = 4.9, 10.36, and 78.39, respectively).

To evaluate the basis set superposition errors (BSSEs) produced in the calculations of the interaction energies between glycinamide (glycinamidic acid) and formamide (formamidic acid), the Boys−Bernardi counterpoise technique has been employed.[66]

All of the computations were performed using the Gaussian 98 program and the SCF convergence criteria *Tight* was used throughout, especially for those single-point energy calculations at the B3LYP/6-311++G** level of theory since the basis set adopted here contains diffuse functions.[67]

3. Results and Discussions

3.1. Structural Features. Table 1 lists the selected geometrical parameters for the complexes of **G**−**F**, **TS**, and **G′**−**F′** together with their rotational constants and dipole moments. Hopefully, the predicted values for those rotational constants

TABLE 1: Selected Geometrical Parameters for Complexes of G−F, TS, and G′−F′ Together with Their Dipole Moments (in Debye) and Rotational Constants (in GHz) Obtained at the B3LYP/6-311++G Level of Theory[a]**

para.	G−F	TS[b]	G′−F′[b]
R(1,2)	1.5313	1.5222(−0.0091)	1.5213(−0.0100)
R(1,4)	1.3390	1.2916(−0.0474)	1.2815(−0.0575)
R(1,5)	1.2355	1.2997(0.0642)	1.3188(0.0833)
R(4,10)	1.0104	1.0180(0.0076)	1.0198(0.0094)
R(4,11)	1.0230	1.3493(0.3263)	1.5885(0.5655)
R(12,13)	1.2264	1.2860(0.0596)	1.3065(0.0801)
R(12,14)	1.3435	1.2973(−0.0462)	1.2846(−0.0589)
R(14,16)	1.0293	1.4586(0.4293)	1.6452(0.6159)
R(14,17)	1.0069	1.0135(0.0066)	1.0150(0.0081)
A(2,1,4)	115.98	122.16(6.18)	124.01(8.03)
A(2,1,5)	119.25	113.69(−5.56)	112.27(−6.98)
A(4,1,5)	124.76	124.15(−0.62)	123.72(−1.05)
A(1,4,11)	120.56	124.58(4.02)	125.94(5.38)
A(1,5,16)	123.20	112.69(−10.51)	111.46(−11.74)
A(13,12,14)	125.28	124.67(−0.62)	124.50(−0.79)
A(11,13,12)	122.05	112.99(−9.05)	111.74(−10.31)
A(12,14,16)	120.41	123.43(3.02)	124.51(4.10)
D(4,1,2,3)	12.58	8.57(−4.01)	9.43(−3.15)
D(5,1,2,3)	−168.36	−171.94(−3.58)	−171.08(−2.72)
D(2,1,4,10)	0.42	0.50(0.08)	0.50(0.08)
D(2,1,4,11)	178.12	179.20(1.08)	178.93(0.81)
D(5,1,4,10)	−178.58	−178.93(−0.35)	−178.93(−0.35)
D(5,1,4,11)	−0.88	−0.23(0.65)	−0.50(0.38)
D(2,1,5,16)	−178.04	−178.21(−0.16)	−178.17(−0.13)
D(4,1,5,16)	0.93	1.27(0.34)	1.32(0.39)
D(1,4,13,12)	0.06	−1.03(−1.09)	−0.63(−0.69)
D(1,5,14,12)	−0.66	−1.72(−1.06)	−1.57(−0.92)
D(14,12,13,11)	0.19	0.40(0.22)	0.20(0.01)
D(15,12,13,11)	−179.81	−179.60(0.21)	−179.80(0.01)
D(13,12,14,16)	0.04	0.45(0.42)	0.45(0.41)
D(15,12,14,16)	−179.97	−179.54(0.42)	−179.56(0.41)
D(15,12,14,17)	−0.03	0.02(0.05)	−0.01(0.03)
A[c]	4.668(−1.92)	4.549(−2.55)	4.521(−1.93)
B	0.818(1.02)	0.954(0.90)	0.907(0.89)
C	0.703(0.32)	0.796(0.27)	0.762(0.33)
dipole moments	2.20	2.72	2.15

[a] All the bond lengths (R), bond angles (A), and dihedral angles (D) are in angstroms and degrees, respectively. [b] The data in parentheses are the geometrical changes relative to **G−F**. [c] The data in parentheses refer to the dipole moments along the principal axes.

and dipole moments should be helpful in the identification or observation of these complexes using the rotational spectroscopy and microwave spectrum experimentally.

As displayed in Figure 1, the selected complexes associated with the DPT are characterized by an eight-membered ring formed through a pair of two parallel intermolecular H-bonds, where all of the eight atoms of the ring are almost planar. Obviously, from the calculated intermolecular distances, one can say that the strength of H-bonds formed in **G−F** is weaker than that formed in **G′−F′**, which can be also reflected from the increasing of the linearity of the H-bond angles of A(O5H16N14) and A(N4H11O13) with the proceeding of PT reaction. Moreover, analyses of the distances between heavy atoms associated with the H-bonds show that the smaller distances of O5−N14 (2.668 Å) and N4−O13 (2.628 Å) in **G′−F′** may be comparable to those of complexes possessing low-barrier H-bonds, implying that the DPT from **G′−F′** to **G−F** should proceed with a lower barrier height according to the characters of the low-barrier H-bonds.[68] Additionally, as an important finding in our previous studies,[56e] the corresponding barrier heights are correlated with the extent to which the angle A(O5C1N4) is bent, that is, the larger the degree of the compression (or expansion) of the A(O5C1N4) is, the higher the barrier height is. Here, the changes of angle A(O5C1N4) for **G−F** and **G′−F′** relative to **TS** are well comparable to those results of PT assisted directly with two water molecules.[56e] Considering the low-barrier heights in the water-assisted case mentioned above, the barrier heights for **G−F** ↔ **G′−F′** tautomeric process should be similar to or even lower than those of the water-assisted case, especially for the reverse reaction.

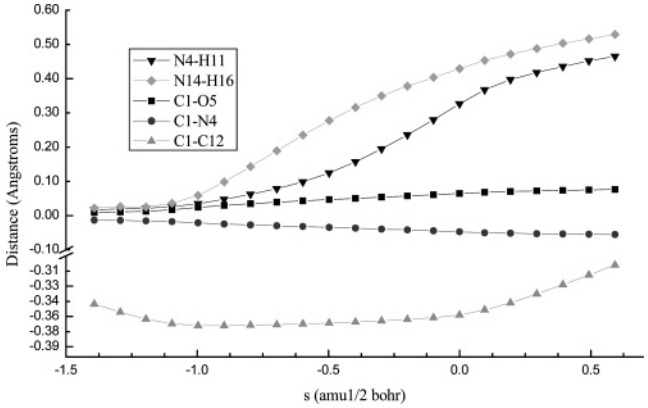

Figure 2. The selected geometrical parameter changes relative to those in optimized **G−F** versus reaction coordinate *s* in the DPT process.

As far as the fragment of glycinamide in **G−F** is concerned, some geometrical changes take place mainly in the regions of intermolecular H-bonds as expected. The double-bond and single-bond characters of the peptide bond C1−N4 and C1−O5 bond have been strengthened, which can be also reflected from their changes versus reaction coordinate qualitatively as illustrated in Figure 2. As expected, the opposite trends can be true for that of glycinamidic acid upon complexation compared with its optimized isolated form. Overall, the geometrical

TABLE 2: The Calculated Interaction Energies, Deformation Energies, BSSE, and ZPVE Corrections for the Interaction of Glycinamide (Glycinamidic Acid) with Formamide (Formamidic Acid)[a]

	G−F	**G′−F′**
ΔE_{inter}[b]	−13.12(−11.22)[−10.78]	−20.68(−19.77)[−18.93]
ΔE_{ZPVE}	1.90	0.90
ΔE_{BSSE}	0.43	0.84
$\Delta E_{defor.}$[c]	0.55(0.59)	3.12(3.95)

[a] All the units are in kcal/mol. [b] The data in parentheses and brackets refer to those with ZPVE and further BSSE corrections, respectively. [c] The data in parentheses refer to those of the formamide and formamidic acid fragments, respectively.

changes for two fragments in **G′−F′** are larger than those in **G−F** partly because of the existence of the stronger intermolecular H-bonds in the former. At the same time, the corresponding changes occurring in the **TS** lie in the mediate between **G−F** and **G′−F′**, reflecting its transitional nature accompanying the PT. Additionally, compared with **G−F** and **G′−F′**, the **TS** resembles **G′−F′** more closely than **G−F**, which is well consistent with Hammond's postulates since the tautomeric process from **G−F** to **G′−F′** is an endothermic reaction as discussed below.[69]

Figure 2 displays the selected geometrical changes associated with the DPT versus reaction coordinates. The concerted mechanism of DPT in nature can be reflected from the changes of two transferring protons, H11 and H16, along the reaction coordinates qualitatively. Hopefully, the changes of intermolecular distance (C1−C2) between two fragments, that is, decreasing first and then increasing, may be helpful in understanding the dynamics of the DPT reactions.

As mentioned below, three complexes have also been fully reoptimized employing the MP2(FULL)/6-311++G** level of theory to further explore the barrier heights due to the disappearance of the barrier height for the reverse reaction with inclusion of ZPVE corrections at the B3LYP/6-311++G** level of theory. Overall, both B3LYP and MP2(FULL) levels can give consistent results with each other, especially for those intermolecular H-bonds as mentioned above. Here, the optimized structures for them are not discussed detailedly since what we most concerns is the energetic features at the MP2(FULL)/6-311++G** level of theory.

3.2. Interaction Energies. Table 2 summarizes the calculated interaction energies produced in the DPT process, where the interaction energy is defined as the energy difference between the optimized complexes and the sums of the optimized monomers including the ZPVE and BSSE corrections.

As displayed in Figure 1, glycinamide (glycinamidic acid) and formamide (formamidic acid) interact with each other through the formation of a pair of two parallel intermolecular H-bonds. For the interaction of glycinamide with formamide, its interaction energy is smaller than that of corresponding glycinamidic acid with formamidic acid, where the interaction energies are −13.12 (−10.78) and −20.68 (−18.93) kcal/mol without (with) ZPVE and BSSE corrections for the former and the latter, respectively. Similar results can be also obtained at the MP2(FULL)/6-311++G** level of theory, where the corresponding values are −12.10 (−9.55) and −19.68 (−16.01) kcal/mol for the former and the latter, respectively. Here, consistent with the above conclusions drawn only from the intermolecular H-bond contact distances, the interaction between glycinamidic acid and formamidic acid is larger than that of glycinamide and formamide. Actually, the strength of the H-bond should belong to the weak (2.4∼12 kcal/mol) and strong (12∼24 kcal/mol) types, respectively, assuming that the classifications of the H-bond strength proposed by Frey et al. hold for the double H-bond.[69] Even so, as described below, the double proton transferred product **G′−F′** is still higher by about 18 kcal/mol in energy than **G−F** since the favorable stability gained from the double H-bond for the former is still too small to predominate over the instability of the isolated glycinamidic acid and formamidic acid relative to glycinamide and formamide intrinsically. Additionally, as listed in Table 2, further inclusions of ZPVE and BSSE corrections lower the interaction energies by about 1.7∼2.3 kcal/mol, relatively smaller than those produced in multiwater-assisted PTs.[56e]

TABLE 3: The Calculated Tautomeric Energies ΔE, ZPVE Corrections, and Barrier Heights ΔE^* for the Forward and Reverse Reactions (Noted with Footnote f and r, Respectively) in the PT Processes[a,b]

	$\Delta E[\Delta H]$	ΔE^*_f	ΔE^*_r
B3LYP	19.75(19.35)[18.83]	20.45(16.98)	0.70(−2.37)
MP2[c]	17.14(16.95)[16.49]	19.12(15.06)	1.98(−1.89)
ΔE_{ZPVE}[d]	−0.40(−0.19)	−3.47(−4.06)	−3.07(−3.87)
MP2[e]	17.37(16.98)	19.13(15.66)	1.75(−1.32)
MP3[e]	15.99(15.59)	19.74(16.27)	3.75(0.68)
MP4SDQ[e]	18.41(18.02)	21.65(18.18)	3.23(0.16)
CCSD(T)[e]	16.57(16.17)	19.27(15.80)	2.70(−0.37)

[a] All the units are in kcal/mol. [b] The data in parentheses refer to those considering ZPVE corrections obtained at the B3LYP/6-311++G** level of theory. [c] All the data obtained at the MP2(FULL)/6-311++G** level of theory with full optimizations including all the electron correlations. [d] The data in parentheses refer to those obtained at the MP2(FULL)/6-311++G** level of theory. [e] The data refer to the single-point energy calculations based on the geometries obtained at the B3LYP/6-311++G** level of theory without and with considering corresponding ZPVE corrections.

Table 2 also presents the calculated deformation energies for the two fragments upon complexation, where the deformation energy is defined as the energy difference between the neutral states at the geometries in the complexes and those in their corresponding optimized isolated states qualitatively. Obviously, the larger deformation energies for the fragments of glycinamidic acid (3.12 kcal/mol) and formamidic acid (3.95 kcal/mol) relative to those of glycinamide (0.55 kcal/mol) and formamide (0.59 kcal/mol) give additional evidence for the larger strength of the intermolecular H-bond in **G′−F′** than in **G−F**.

Additionally, the larger interaction between glycinamidic acid and formamidic acid can also be further reflected from the viewpoint of the ability of the proton acceptor and donor. For example, the O5 (351.99 kcal/mol) and O13 (348.42 kcal/mol) in **G′−F′** are better proton donors than N4 (367.63 kcal/mol) and N14 (361.62 kcal/mol) in **G−F**, where the data in parentheses refer to the calculated proton affinities at the B3LYP/6-311++G** level of theory and the larger PAs for the deprotonated (neutral) species stand for a weak acid (strong base). Moreover, the ability of the proton acceptor at N4 (222.65 kcal/mol) and N14 (205.94 kcal/mol) in **G′−F′** is also stronger than O5 (209.5 kcal/mol) and O13 (192.74 kcal/mol) in **G−F**.

3.3. DPT Process. *3.3.1. Thermodynamics.* As listed in Table 3, the tautomeric energy from **G−F** to **G′−F′** is 19.75 and 19.35 kcal/mol before and after considering ZPVE corrections, indicating the stability of **G−F** relative to **G′−F′**. This point can be further reflected from the calculated potential energy curves versus reaction coordinate *s* as depicted in Figure 6 qualitatively. At the same time, ZPVE corrections have a little influence on the tautomerism though inclusion of them slightly favors the tautomerism. Compared with those direct tautomeric processes occurring in both monomers,[56e] the present value is

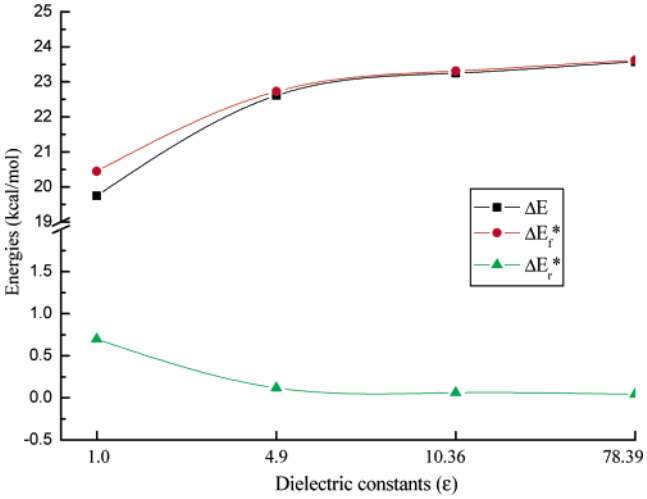

Figure 3. The dependences of the forward, the reverse barrier heights, and the tautomeric energy changes on various dielectric constants in the DPT process.

larger than either of them, where the tautomeric energies for glycinamide and formamide are 14.44 and 13.47 kcal/mol with ZPVE corrections at the B3LYP/6-311++G** level of theory. Thus, the participation of a formamide molecule should disfavor the tautomeric process from the thermodynamic point of view. On the other hand, the reductions of about 8.56 kcal/mol for the tautomeric energy relative to the sums of those two monomers should be due to the different H-bond strengths between **G**−**F** and **G′**−**F′** as mentioned by Kim et al.[17e] Qualitatively, in solution, the dependence of the tautomeric energy on the dielectric constants has been illustrated in Figure 3 on the basis of the IPCM model within the framework of the SCRF theory. Obviously, the presence of bulk solvent slightly increases the tautomeric energy relative to that in the gas phase though the increments are relatively small with the increasing of dielectric constants. These change trends can be understood since the solvation energies are slightly favorable to **G**−**F** over **G′**−**F′**, which is consistent with the fact that the former has a slightly larger dipole moment (2.20 D) than the latter (2.15 D) as listed in Table 1.

As shown in Table 3, the positive values of enthalpy changes indicate that the tautomeric process should be an endothermic reaction, where the ΔH (18.83 kcal/mol) at the B3LYP/6-311++G** level of theory is comparable to that of 16.49 kcal/mol at the MP2(FULL)/6-311++G** level of theory. The calculated relatively small values for ΔS (−4.7 cal/mol-K) show that the ΔG should be essentially governed by ΔH in the tautomeric process. According to the Boltzmann statistics, that is, $K_p = \exp[-\Delta G°/(RT)]$, the calculated equilibrium constant is 1.51×10^{-15} at 298.15 K and 1.0 atm, which is smaller than those direct and water-assisted cases ranging from 2.37×10^{-11} to 5.99×10^{-10}.[56e]

To improve the calculated energy quantities, we have also carried out the single-point energy calculations employing the MP2, MP3, MP4SDQ, and CCSD(T) levels including all the electron correlations on the basis of the geometries obtained at the B3LYP/6-311++G** level of theory. Obviously, the calculated tautomeric energy is overestimated about 0.81∼3.24 kcal/mol at the B3LYP level relative to these higher levels. Similarly, the same observation is also true for the comparisons with that obtained with the full optimizations at the MP2(FULL)/6-311++G** level of theory. Interestingly, the well-consistent results can be obtained between the single-point energy calculation and full optimizations at the same level of MP2(FULL).

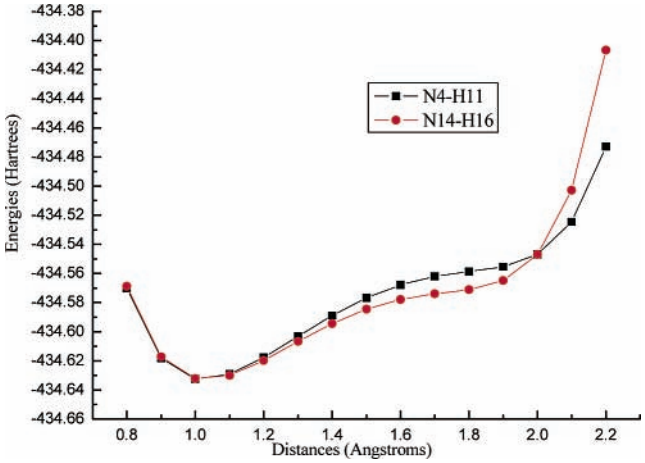

Figure 4. The calculated potential energy surfaces along the N4−H11 and N14−H16 bonds of **G**−**F**.

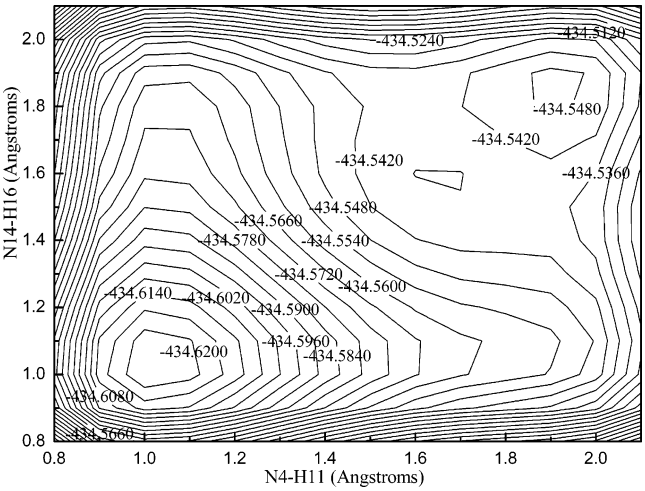

Figure 5. Two-dimensional PES sections obtained by scanning the N4−H11 and N14−H16 bonds in **G**−**F**.

For example, the difference in tautomeric energy between them is only 0.23 kcal/mol and inclusions of the ZPVE corrections further reduce the difference to 0.03 kcal/mol, where the ZPVE corrections used for single-point energy calculations are those obtained at the B3LYP level. As discussed below, the same conclusions also hold for those calculated barrier heights.

3.3.2 Kinetics. First of all, using the optimized **G**−**F** as an initial geometry, we scan, respectively, the N4−H11 and N14−H16 bonds without optimizing the remaining parameters to better understand the DPT mechanism (concerted or stepwise). The schematic potential energy curves along these two bonds have been illustrated in Figure 4. Obviously, both of them assume a single-well potential though an inflection point appears in the vicinity of between 1.6 and 1.8 Å. Actually, those ion-pair structures resulting from the stepwise mechanism have collapsed to **G**−**F** during the full optimizations. Thus, the stepwise mechanism for the DPT has been excluded. Furthermore, the two-dimensional PES has been constructed through only scanning the N4−H11 and N14−H16 bonds simultaneously without optimizing the remaining parameters since it is too expensive to do so presently to the best of our ability. As displayed in Figure 5, there are two minima separated by a saddle point (**TS**). Qualitatively, both minima are located at about (1.02, 1.02) and (1.9, 1.9) nearby, corresponding to the **G**−**F** and **G′**−**F′**, respectively. As mentioned above, the location of the **TS** is close to that of the **G′**−**F′**. Intuitively, the barrier

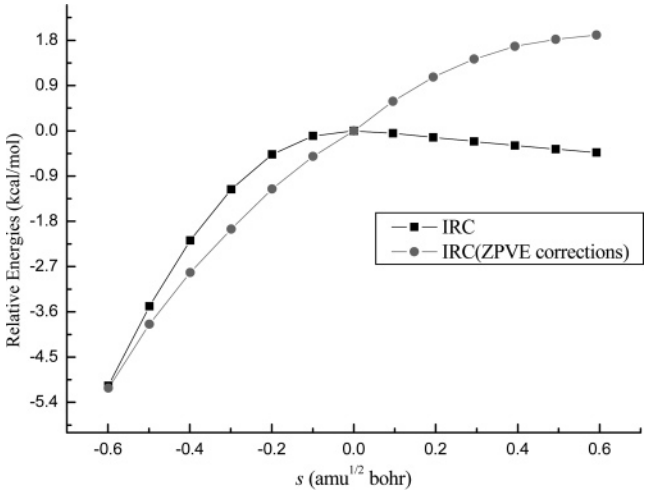

Figure 6. The calculated potential energy curves relative to optimized **TS** versus reaction coordinate *s* in the DPT process.

height from **G′−F′** to **TS** should be very small though the relaxed PES should be required to further confirm this point.

As listed in Table 3, the barrier heights in the forward and reverse directions are 20.45 and 0.70 kcal/mol, respectively. Interestingly, both of them have been reduced by about 3.47 and 3.07 kcal/mol to 16.98 and −2.37 kcal/mol with further inclusions of ZPVE corrections. Here, the disappearance of the reverse barrier height suggests that **G′−F′** should be converted to **G−F** instantaneously once **G′−F′** is produced and the reverse barrier height is low enough that the ZPVE level is above the barrier, which is analogues to the representative low-barrier H-bonds.[70] Furthermore, this point can be reflected from the calculated potential energy curves along the reaction coordinate. As displayed in Figure 6, the energies of the nonstationary points in the vicinity of the products are slightly lower than that of the **TS** without considering ZPVE corrections. However, the case is opposite if considering ZPVE corrections through calculating the frequencies of those nonstationary points approximately. Obviously, as described above, the product is higher in energy than **TS,** implying the key role of ZPVE corrections in controlling the proceeding of the reverse reaction. In fact, the energy level of the unique imaginary frequency of the **TS** (766.7i cm^{-1} versus 2.19 kcal/mol) is also higher than that of non-ZPVE-corrected reverse barrier height (0.70 kcal/mol), but it is much lower than that of forward barrier height. Thus, in a sense, the lack of a vibrational degree of freedom in **TS** (corresponding to its imaginary frequency) makes the ZPVE corrections favorable to **TS** relative to **G′−F′** since both of them have similar geometries as mentioned above. Compared with those direct PTs in glycinamide and formamide, the barrier heights in **G−F** have been reduced significantly, especially for the reverse reaction, where the forward (reverse) barrier heights in the isolated states are 45.36 (30.93) and 45.41 (31.93) kcal/mol at the B3LYP/6-311++G** level of theory for the former and the latter, respectively. This point is well consistent with the slight changes for A(N4C1O5) from **G′−F′** to **TS** as mentioned above. The forward barrier height can be comparable to that of two-water-assisted cases since both of them have similar changes for the A(N4C1O5) from the reactant to **TS** (0.62° versus 0.14°).[56e]

Considering the fact that the disappearance of the barrier height may be an artificial product of the method adopted here, we have reoptimized these structures employing the MP2-(FULL)/6-311++G** level of theory though it is much more expensive relative to B3LYP level for the study of glycinamide

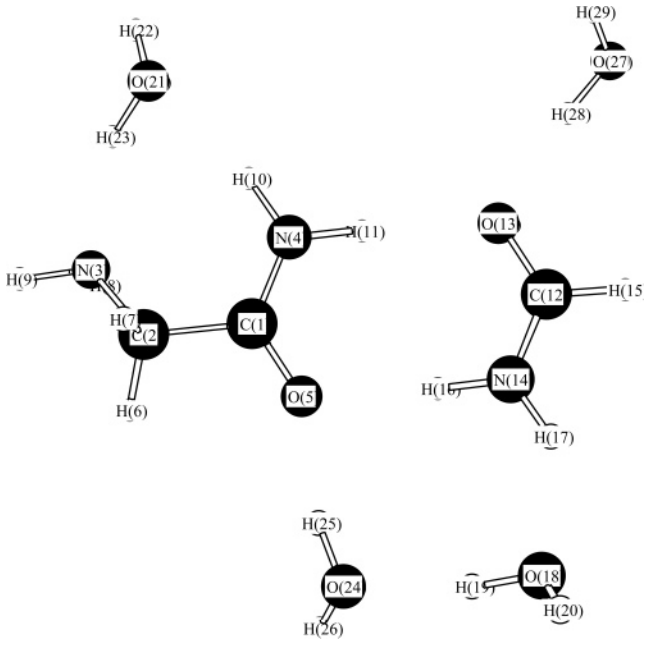

Figure 7. Selected hydrated **G−F** complex with four water molecules at the B3LYP/6-311++G** level of theory.

complexes applied here. As listed in Table 3, the barrier heights for the forward and reverse reactions have been changed to 19.12 (15.06) and 1.98 (−1.89) kcal/mol without (with) considering ZPVE corrections at the MP2(FULL)/6-311++G** level of theory, where the reverse barrier height has disappeared once again. Thus, the reliability of B3LYP level in predicting the barrier heights for glycinamide complexes has been further confirmed though it overestimates (underestimates) them about 1.92 (0.48) kcal/mol for the forward (reverse) reaction compared with those obtained at the MP2(FULL) level. On the other hand, applications of the ZPVE corrections obtained at the B3LYP level to those higher-level single-point energy calculations also make the reverse barrier height disappear except for MP3 and MP4SDQ levels. However, if the ZPVE corrections obtained at the MP2(FULL) level are applied, both levels also make the reverse barrier height disappear since the ZPVE corrections in absolute value at the MP2(FULL) level are greater than those at the B3LYP level. In fact, the disappearances of the barrier heights have also been reported previously for the different systems.[17f,18a,29e,43−47] Of course, more accurate computations are required to further confirm this point. Additionally, the consistent results between those of the single-point energy calculation with and without ZPVE corrections obtained at the B3LYP level and those of the full optimizations can be observed again at the same MP2(FULL) level as mentioned above.

As displayed in Figure 3, the solvent effects on the barrier heights have been evaluated qualitatively employing the IPCM model on the basis of the optimized gas-phase geometries. Overall, the existences of bulk solvent have only slight influences on the barrier heights, where the largest changes in aqueous solution are about 3.42 and −0.66 kcal/mol for the forward and reverse reactions compared with those in the gas phase. As expected, the reverse barrier height decreases with the increasing of dielectric constants, which is well correlated with the fact that the **TS** has a larger dipole moment (2.72 D) relative to **G′−F′** (2.15 D). Unexpectedly, the opposite changing trend appears for the forward barrier height, which cannot be elucidated solely from the size of the dipole moments since the dipole moment of **G−F** (2.20 D) is smaller than that of **TS**. Probably, other factors, such as local dipoles and higher

multipole moments, should play an important role for the solvent stabilization of **G**−**F**. Thus, the presence of bulk solvent may be more favorable for the existence of **G**−**F** relative to **G′**−**F′**. Furthermore, as a preliminary study, the DPT behavior of hydrated **G**−**F** complex with four water molecules has been investigated at the B3LYP/6-311++G** level of theory. As displayed in Figure 7, full optimizations reveal that only the nonproton-transferred structure has been localized during the DPT process; in other words, neither of the protons, H11 and H16, can be transferred between two fragments, implying the favorable stability of **G**−**F** because of the existence of the explicit interactions with adjacent water molecules. Considering the complexity of the DPT behaviors in realistic biological medium for these complexes, we expect that more extensive investigations should be required in the future with more accurate solvation models.

4. Conclusions

In the present paper, DPT process occurring between two model peptide fragments, that is, glycinamide and formamide, has been investigated employing the B3LYP/6-311++G** level of theory. Thermodynamic and especially kinetic parameters, such as tautomeric energy, equilibrium constant, and barrier heights, have been discussed, respectively. The relevant quantities involved in the DPT process, such as geometrical changes, interaction energies, and intrinsic reaction coordinate (IRC) calculations, have also been studied. The principal conclusions from this study are as follows:

1. Thermodynamically, contrary to those tautomeric processes directly assisted with one, two, and three water molecules,[56e] the participation of a formamide molecule disfavors the tautomeric process for both glycinamide and formamide compared with their direct tautomeric cases, where the tautomeric energy from **G**−**F** to **G′**−**F′** is larger by about 4.91 and 5.88 kcal/mol than those of glycinamide and formamide, respectively.

2. The DPT process from **G**−**F** to **G′**−**F′** should proceed with a concerted mechanism rather than a stepwise one since no ion-pair complexes have been located during the PT process.

3. The barrier heights are 20.45 and 0.70 kcal/mol for the forward and reverse directions at the B3LYP/6-311++G** level of theory. However, both of them have been reduced by 3.47 and 3.07 kcal/mol to 16.98 and −2.37 kcal/mol with further inclusion of ZPVE corrections, respectively. Moreover, this phenomenon has been reproduced by the similar barrier height (−1.89 (1.98) kcal/mol with and without considering ZPVE corrections) at the MP2(FULL)/6-311++G** level of theory, indicating the importance of the ZPVE corrections. These observations have also implied that although a minimum can be located for **G′**−**F′** theoretically, the actual DPT from **G′**−**F′** to **G**−**F** is thermodynamically spontaneous, a barrierless process. Additionally, applications of the IPCM model within the framework of the SCRF theory indicate that the existence of bulk solvent has a subtle influence on the tautomeric energy and barrier heights.

4. The good agreement between B3LYP/6-311++G** and higher levels further confirms the reliability of the B3LYP/6-311++G** level of theory in exploring the DPT phenomena, paving the way for future studies on the DPT behaviors in glycinamide complexes employing it.

Acknowledgment. This work is supported by the National Natural Science Foundation of China (20273040) and the Natural Science Foundation of Shandong Province (Key project), and the support from SRFDP and the Foundation for University Key Teacher by the Ministry of Education of China is also acknowledged. We are also grateful to the referees for their excellent suggestions to improve the presentation of the results.

References and Notes

(1) Desiraju, G. R. *Acc. Chem. Res.* **1991**, *24*, 290.
(2) Hibbert, F. *Adv. Phys. Org. Chem.* **1986**, *22*, 113.
(3) Beeman, R. W.; Matsumura, F. *Nature* **1973**, *242*, 274.
(4) Zhang, K.; Chung-Phillips, A. *J. Chem. Inf. Comput. Sci.* **1999**, *39*, 382.
(5) (a) Gorb, L.; Leszczynski, J. *Int. J. Quantum Chem.* **1998**, *70*, 855. (b) Venkateswarlu, D.; Leszczynski, J. *J. Phys. Chem. A* **1998**, *102*, 6161. (c) Gorb, L.; Leszczynski, J. *J. Am. Chem. Soc.* **1998**, *120*, 5024. (d) Gu, J.; Leszczynski, J. *J. Phys. Chem. A* **1999**, *103*, 577. (e) Gu, J.; Leszczynski, J. *J. Phys. Chem. A* **1999**, *103*, 2744. (f) Zhanpeisov, N. U.; Cox, W. W., Jr.; Leszczynski, J. *J. Phys. Chem. A* **1999**, *103*, 4564. (g) Shukla, M. K.; Leszczynski, J. *J. Phys. Chem. A* **2000**, *104*, 3021. (h) Podolyan, Y.; Gorb, L.; Leszczynski, J. *J. Phys. Chem. A* **2002**, *106*, 12103. (i) Gorb, L.; Podolyan, Y.; Leszczynski, J.; Siebrand, W.; Fernández-Ramos, A.; Smedarchina, Z. *Biopolymers* **2002**, *61*, 77. (j) Zhanpeisov, N. U.; Leszczynski, J. *J. Phys. Chem. A* **1999**, *103*, 8317. (k) Leszczynski, J. *J. Phys. Chem. A* **1998**, *102*, 2357.
(6) Wang, X.; Nichols, J.; Feyereisen, M.; Gutowski, M.; Boatz, J.; Haymet, A. D. J.; Simons, J. *J. Phys. Chem.* **1991**, *95*, 10419.
(7) (a) Bell, R. L.; Taveras, D. L.; Truong, T. N.; Simons, J. *Int. J. Quantum Chem.* **1997**, *63*, 861. (b) Bell, R. L.; Truong, T. N. *J. Chem. Phys.* **1994**, *101*, 10442. (c) Zhang, Q.; Bell, R.; Truong, T. N. *J. Phys. Chem.* **1995**, *99*, 592.
(8) Jensen, J. H.; Gordon, M. S. *J. Am. Chem. Soc.* **1995**, *117*, 8159.
(9) Król-Starzomska, I.; Filarowski, A.; Rospenk, M.; Koll, A.; Melikova, S. *J. Phys. Chem. A* **2004**, *108*, 2131.
(10) (a) Scheiner, S.; Kern, C. W. *J. Am. Chem. Soc.* **1979**, *101*, 4081. (b) Scheiner, S.; Wang, L. *J. Am. Chem. Soc.* **1993**, *115*, 1958. (c) Scheiner, S. *J. Am. Chem. Soc.* **1981**, *103*, 315. (d) Scheiner, S.; Redfern, R.; Szczesniak, M. M. *J. Phys. Chem.* **1985**, *89*, 262. (e) Scheiner, S.; Harding, L. B. *J. Am. Chem. Soc.* **1981**, *103*, 2169.
(11) (a) Bertran, J.; Oliva, A.; Rodríguez-Santiago, L.; Sodupe, M. *J. Am. Chem. Soc.* **1998**, *120*, 8159. (b) Rodríguez-Santiago, L.; Sodupe, M.; Oliva, A.; Bertran, J. *J. Am. Chem. Soc.* **1999**, *121*, 8882.
(12) Pranata, J.; Davis, G. D. *J. Phys. Chem.* **1995**, *99*, 14340.
(13) (a) Nguyen, K. A.; Gordon, M. S.; Truhlar, D. G. *J. Am. Chem. Soc.* **1991**, *113*, 1596. (b) Gordon, M. S. *J. Phys. Chem.* **1996**, *100*, 3974. (c) Chaban, G. M.; Gordon, M. S. *J. Phys. Chem. A* **1999**, *103*, 185. (d) Petrich, J. W.; Gordon, M. S.; Cagle, M. *J. Phys. Chem. A* **1998**, *102*, 1647.
(14) Wu, D. H.; Ho, J. J. *J. Phys. Chem. A* **1998**, *102*, 3582.
(15) Yen, S. J.; Lin, C. Y.; Ho, J. J. *J. Phys. Chem. A* **2000**, *104*, 11771.
(16) Rodriquez, C. F.; Cunje, A.; Shoeib, T.; Chu, I. K.; Hopkinson, A. C.; Siu, K. W. M. *J. Phys. Chem. A* **2000**, *104*, 5023.
(17) (a) Kim, Y. *J. Am. Chem. Soc.* **1996**, *118*, 1522. (b) Lim, J.-H.; Lee, E. K.; Kim, Y. *J. Phys. Chem. A* **1997**, *101*, 2233. (c) Kim, Y.; Hwang, H. J. *J. Am. Chem. Soc.* **1999,** *121*, 4669. (d) Kim, Y. *J. Phys. Chem. A* **1998,** *102*, 3025. (e) Kim, Y.; Lim, S.; Kim, H.-J.; Kim, Y. *J. Phys. Chem. A* **1999**, *103*, 617. (f) Kim, Y.; Lim, S.; Kim, Y. *J. Phys. Chem. A* **1999**, *103*, 6632.
(18) (a) Florián, J.; Hrouda, V.; Hobza, P. *J. Am. Chem. Soc.* **1994**, *116*, 1457. (b) Hrouda, V.; Florián, J.; Polášek, M.; Hobza, P. *J. Phys. Chem.* **1994**, *98*, 4742. (c) Florián, J.; Leszczyński, J. *J. Am. Chem. Soc.* **1996**, *118*, 3010.
(19) Minyaev, R. M. *Chem. Phys. Lett.* **1996**, *262*, 194.
(20) Adamo, C.; Cossi, M.; Barone, V. *J. Comput. Chem.* **1997**, *18*, 1993.
(21) Pan, Y.; McAllister, M. A. *J. Am. Chem. Soc.* **1997**, *119*, 7561.
(22) Lu, D.; Voth, G. A. *J. Am. Chem. Soc.* **1998**, *120*, 4006.
(23) Kryachko, E. S.; Nguyen, M. T. *J. Phys. Chem. A* **2001**, *105*, 153.
(24) Chaudhuri, C.; Jiang, J. C.; Wu, C.-C.; Wang, X.; Chang, H.-C. *J. Phys. Chem. A* **2001**, *105*, 8906.
(25) Taylor, J.; Eliezer, I.; Sevilla, M. D. *J. Phys. Chem. B* **2001**, *105*, 1614.
(26) Tatara, W.; Wójcik, M. J.; Lindgren, J.; Probst, M. *J. Phys. Chem. A* **2003**, *107*, 7827.
(27) Cui, Q.; Karplus, M. *J. Phys. Chem. B* **2003**, *107*, 1071.
(28) Kulhánek, P.; Schlag, E. W.; Koča, J. *J. Am. Chem. Soc.* **2003**, *125*, 13678.
(29) (a) Chou, P.-T.; Yu, W.-S.; Chen, Y.-C.; Wei, C.-Y.; Martinez, S. S. *J. Am. Chem. Soc.* **1998**, *120*, 12927. (b) Chou, P.-T.; Wu, G.-R.; Wei, C.-Y.; Cheng, C.-C.; Chang, C.-P.; Hung, F.-T. *J. Phys. Chem. B* **1999**, *103*, 10042. (c) Chou, P.-T.; Wei, C.-Y.; Chris Wang, C.-R.; Hung, F.-T.; Chang, C.-P. *J. Phys. Chem. A* **1999**, *103*, 1939. (d) Chou, P.-T.; Wu, G.-R.; Wei, C.-Y.; Cheng, C.-C.; Chang, C.-P.; Hung, F.-T. *J. Phys. Chem. B* **2000**, *104*, 7818. (e) Hung, F.-T.; Hu, W.-P.; Li, T.-H.; Cheng, C.-C.; Chou, P.-T. *J. Phys. Chem. A* **2003**, *107*, 3244.

(30) Kryachko, E. S.; Nguyen, M. T.; Zeegers-Huyskens, T. *J. Phys. Chem. A* **2001**, *105*, 1934.
(31) Graf, F.; Meyer, R.; Ha, T.-K.; Ernst, R. R. *J. Chem. Phys.* **1981**, *75*, 2914.
(32) Mitra, S.; Das, R.; Bhattacharyya, S. P.; Mukherjee, S. *J. Phys. Chem. A* **1997**, *101*, 293.
(33) Glaser, R.; Lewis, M. *Org. Lett.* **1999**, *1*, 273.
(34) Brinkmann, N. R.; Tschumper, G. S.; Yan, G.; Schaefer, H. F., III. *J. Phys. Chem. A* **2003**, *107*, 10208.
(35) Moreno, M.; Douhal, A.; Lluch, J. M.; Castano, O.; Frutos, L. M. *J. Phys. Chem. A* **2001**, *105*, 3887.
(36) Clementi, E.; Mehl, J.; Niessen, W. V. *J. Chem. Phys.* **1971**, *54*, 508.
(37) Del Bene, J. E.; Kochenour, W, L. *J. Am. Chem. Soc.* **1976**, *98*, 2041.
(38) Schweiger, S.; Rauhut, G. *J. Phys. Chem. A* **2003**, *107*, 9668.
(39) Ahn, D.-S.; Park, S.-W.; Jeon, I.-S.; Lee, M.-K.; Kim, N.-H.; Han, Y.-H.; Lee, S. *J. Phys. Chem. B* **2003**, *107*, 14109.
(40) Hayashi, S.; Umemura, J.; Kato, S.; Morokuma, K. *J. Phys. Chem.* **1984**, *88*, 1330.
(41) Barone, V.; Adamo, C. *J. Phys. Chem.* **1995**, *99*, 15062.
(42) Yamabe, T.; Yamashita, K.; Kaminoyama, M.; Koizumi, M.; Tachibana, A.; Fukui, K. *J. Phys. Chem.* **1984**, *88*, 1459.
(43) Guallar, V.; Douhal, A.; Moreno, M.; Lluch, J. M. *J. Phys. Chem. A* **1999**, *103*, 6251.
(44) Makowski, M.; Liwo, A.; Wrobel, R.; Chmurzynski, L. *J. Phys. Chem. A* **1999**, *103*, 11104.
(45) Norikane, Y.; Nakayama, N.; Tamaoki, N.; Arai, T.; Nagashima, U. *J. Phys. Chem. A* **2003**, *107*, 8659.
(46) Park, S.-W.; Ahn, D.-S.; Lee, S. *Chem. Phys. Lett.* **2003**, *371*, 74.
(47) Shimoni, L.; Glusker, J. P.; Bock, C. W. *J. Phys. Chem.* **1996**, *100*, 2957.
(48) Oie, T.; Loew, G. H.; Burt, S. K.; MacElroy, R. D. *J. Am. Chem. Soc.* **1984**, *106*, 8007.
(49) Jensen, J. H.; Baldridge, K. K.; Gordon, M. S. *J. Phys. Chem.* **1992**, *96*, 8340.
(50) (a) Remko, M.; Rode, B. M. *Chem. Phys. Lett.* **2000**, *316*, 489. (b) Remko, M.; Rode, B. M. *Phys. Chem. Chem. Phys.* **2001**, *3*, 4667.
(51) Klassen, J. S.; Kebarle, P. *J. Am. Chem. Soc.* **1997**, *119*, 6552.
(52) Kinser, R. D.; Ridge, D. P.; Hvistendahl, G.; Rasmussen, B.; Uggerud, E. *Chem. —Eur. J.* **1996**, *2*, 1143.
(53) Sulzbach, H. M.; Schleyer, P. V. R.; Schaefer, H. F., III. *J. Am. Chem. Soc.* **1994**, *116*, 3967.
(54) Ramek, M.; Cheng, V. K. W. *Int. J. Quantum Chem., Quantum Boil. Symp.* **1992**, *19*, 15.
(55) Grewal, R. N.; Aribi, H. E.; Smith, J. C.; Rodriquez, C. F.; Hopkinson, A. C.; Siu, K. W. M. *Int. J. Mass Spectrom.* **2002**, *219*, 89.
(56) (a) Li, P.; Bu, Y.; Ai, H. *J. Phys. Chem. A* **2003**, *107*, 6419. (b) Li, P.; Bu, Y.; Ai, H. *J. Phys. Chem. B* **2004**, *108*, 1405. (c) Li, P.; Bu, Y.; Ai, H. *J. Phys. Chem. A* **2004**, *108*, 4069. (d) Li, P.; Bu, Y.; Ai, H. *J. Phys. Chem. A* **2004**, *108*, 1200. (e) Li, P.; Bu, Y. *J. Phys. Chem. B*, in revision.
(57) Johnson, B. G.; Gill, P. M. W.; Pople, J. A. *J. Chem. Phys.* **1993**, *98*, 5612.
(58) (a) Gonzalez, C.; Schlegel, H. B. *J. Chem. Phys.* **1989**, *90*, 2154. (b) Gonzalez, C.; Schlegel, H. B. *J. Phys. Chem.* **1990**, *94*, 5523.
(59) Becke, A. D. *J. Chem. Phys.* **1993**, *98*, 5648.
(60) Lee, C.; Yang, W.; Parr, R. G. *Phys. Rev. B* **1988**, *37*, 785.
(61) (a) Barone, V.; Cossi, M.; Tomasi, J. *J. Comput. Chem.* **1998**, *19*, 404. (b) Barone, V.; Cossi, M. *J. Phys. Chem. A* **1998**, *102*, 1995.
(62) Foresman, J. B.; Keith, T. A.; Wiberg, K. B.; Snoonian, J.; Frisch, M. J. *J. Phys. Chem.* **1996**, *100*, 16098.
(63) (a) Li, X.; Sevilla, M. D.; Sanche, L. *J. Am. Chem. Soc.* **2003**, *125*, 8916. (b) Li, X.; Sanche, L.; Sevilla, M. D. *J. Phys. Chem. A* **2002**, *106*, 11248.
(64) Lee, I.; Kim, C. K.; Han, I. S.; Lee, H. W.; Kim, W. K.; Kim, Y. B. *J. Phys. Chem. B* **1999**, *103*, 7302.
(65) Kovacevic, B.; Maksic, Z. B. *Org. Lett.* **2001**, *3*, 1523.
(66) Boys, S. F.; Bernardi, F. *Mol. Phys.* **1970**, *19*, 553.
(67) Frisch, M. J.; Trucks, G. W.; Schlegel, H. B.; Scuseria, G. E.; Robb, M. A.; Cheeseman, J. R.; Zakrzewski, V. G.; Montgomery, J. A., Jr.; Stratmann, R. E.; Burant, J. C.; Dapprich, S.; Millam, J. M.; Daniels, A. D.; Kudin, K. N.; Strain, M. C.; Farkas, O.; Tomasi, J.; Barone, V.; Cossi, M.; Cammi, R.; Mennucci, B.; Pomelli, C.; Adamo, C.; Clifford, S.; Ochterski, J.; Petersson, G. A.; Ayala, P. Y.; Cui, Q.; Morokuma, K.; Malick, D. K.; Rabuck, A. D.; Raghavachari, K.; Foresman, J. B.; Cioslowski, J.; Ortiz, J. V.; Stefanov, B. B.; Liu, G.; Liashenko, A.; Piskorz, P.; Komaromi, I.; Gomperts, R.; Martin, R. L.; Fox, D. J.; Keith, T.; Al-Laham, M. A.; Peng, C. Y.; Nanayakkara, A.; Gonzalez, C.; Challacombe, M.; Gill, P. M. W.; Johnson, B.; Chen, W.; Wong, M. W.; Andres, J. L.; Gonzalez, C.; Head-Gordon, M.; Replogle, E. S.; Pople, J. A. *Gaussian 98*, revision A.9; Inc., Pittsburgh, PA, 1998.
(68) Frey, P. A.; Whitt, S. A.; Tobin, J. B. *Science* **1994**, *264*, 1927.
(69) Hammond, G. S. *J. Am. Chem. Soc.* **1955**, *77*, 334.
(70) Cleland, W. W.; Kreevoy, M. M. *Science* **1994**, *264*, 1887.